PCCP

Cite this: *Phys. Chem. Chem. Phys.*, 2012, **14**, 11904–11909

www.rsc.org/pccp

PAPER

Synthesis and enhanced electrochemical performance of Li_2CoPO_4F cathodes under high current cycling†

S. Amaresh,[a] G. J. Kim,[a] K. Karthikeyan,[a] V. Aravindan,[ab] K. Y. Chung,[c] B. W. Cho[c] and Y. S. Lee*[a]

Received 26th March 2012, Accepted 13th July 2012
DOI: 10.1039/c2cp41624g

Lithium cobalt fluorophosphate, Li_2CoPO_4F, is successfully synthesized by a solid state reaction under Ar flow at 700 °C. X-ray diffraction and scanning electron microscopic studies are utilized to analyze the structural and morphological features of the synthesized materials, respectively. The presence of fluorine is also supported by energy-dispersive X-ray spectroscopy. The electrochemical properties are evaluated by means of Li/Li_2CoPO_4F half-cell configurations in both potentiostatic and galvanostatic modes. The Li/Li_2CoPO_4F cell delivers an initial discharge capacity of 132 mA h g^{-1} at a current density of 0.1 mA cm^{-2} between 2.0 and 5.1 V at room temperature. Due to the higher operating potential of the $Co^{2+/3+}$ couple in the fluorophosphate matrix, this cell shows a capacity retention of only 53% after 20 cycles, still the material delivered 108 mA h g^{-1} at a high current rate of 1 C. Cyclic voltammetric studies corroborate the insertion and extraction of Li^+ ions by a single phase reaction mechanism during cycling.

Introduction

Energy storage devices such as rechargeable batteries, super-capacitors and fuel cells have gained much attention in recent years, particularly lithium-ion batteries, due to their high energy density (both volumetric and gravimetric), light weight, lowest self-discharge when compared to other rechargeable systems and no memory effect.[1–4] The development of high voltage cathodes for such batteries is necessary to enable them to be used in high energy density power packs and applications such as electric vehicles (EVs), hybrid electric vehicles (HEVs) and plug-in hybrid electric vehicles (P-HEVs).[5] Since the discovery and evaluation of the electrochemical properties of olivine $LiFePO_4$ by Padhi *et al.*,[6] numerous research works have been reported on such polyanion framework materials and they have been commercialized as well. After the success story of $LiFePO_4$, the focus has been directed towards other polyanion framework materials, particularly $(PO_4)^{3-}$ based anions, because of their salient features, such as their ease of synthesis, stability and flat discharge profiles that render high thermal stability.[7–11] Cathode materials based on fluorophosphates can also be considered to be high energy electrode materials, due to the presence of highly electronegative F^- ions which provide much more stability than their counterpart oxygen ions. These fluorophosphate materials possess a 3D-framework structure in which the M–F bonds have higher ionicity than M–O bonds and, hence, the $M^{n/n+1}$ redox couple is expected to exhibit a higher potential than phosphates.[12–15] So far, only a few fluorophosphates have been explored as potential candidates for lithium batteries, including $LiVPO_4F$,[16] $Li_5V(PO_4)_2F_2$,[17] $LiFePO_4F$,[18] $LiTiPO_4F$[19] Li_2MnPO_4F[20] and Na_2FePO_4F.[21] Fluorophosphates have the general formula A_2MPO_4F (A = Li, Na and M = Fe, Mn, Co, Ni) and crystallize in three different forms based on the connectivity of the MO_4F_2 octahedral units, *viz.* face-shared (Na_2FePO_4F), edge-shared (Li_2MPO_4F, M = Co, Ni) and corner-shared (Na_2MnPO_4F). The electrochemical activity of Li_2FePO_4F is found to be 0.85 Li per formula unit, which could be reversibly inserted at ~3.5 V *vs.* Li and its structure is analogous to that of Na_2FePO_4F.[13] Li_2CoPO_4F is also one of the prospective candidates in the fluorophosphate family and shows an electrochemical activity of ~5 V *vs.* Li, which is higher than that of its native compound, $LiCoPO_4$ (4.8 V *vs.* Li).[22–25] Li_2CoPO_4F also possesses the highest redox potential among the currently available cathodes, which makes it an attractive candidate for high-energy density lithium-ion power packs, if high voltage electrolyte problem is resolved.[26–28] Moreover, the theoretical capacity of this material is as high as 287 mA h g^{-1} for the reversible insertion and extraction of two lithium ions per formula unit.

[a] *Faculty of Applied Chemical Engineering, Chonnam National University, Gwang-ju 500-757, Korea. E-mail: leeys@chonnam.ac.kr; Fax: +82 62 530 1904; Tel: +82 62 530 1904*
[b] *Energy Research Institute @ NTU (ERI@N), Nanyang Technological University, Research Techno Plaza, 50 Nanyang Drive, Singapore 637553. E-mail: aravind_van@yahoo.com*
[c] *Center for Energy Convergence, Korea Institute of Science and Technology, Seoul 136-791, Korea*
† Electronic supplementary information (ESI) available. See DOI: 10.1039/c2cp41624g

On the other hand, the main challenge in utilizing such high voltage candidates in practical batteries is the restrictions imposed by the conventional electrolytes.[29] Furthermore, the possibility of utilizing the $Co^{3+/4+}$ redox couple is also questionable for the same reason, which renders the extraction of the two available lithium ions impossible.[22] Also, the cycling performance and electrochemical properties reported so far remain insufficient for practical lithium batteries. Hence, in this study, an attempt was made to synthesize Li_2CoPO_4F cathodes using the conventional solid state method. The particle size of the synthesized Li_2CoPO_4F particles was reduced by planetary ball milling. A high voltage and safer electrolyte was also utilized to evaluate the electrochemical performance of the synthesized Li_2CoPO_4F. Furthermore, rate performance and cyclic voltammetric studies are also conducted and described in detail.

Experimental

Li_2CoPO_4F material was synthesized by the conventional solid state route in a two-step process. First, $LiCoPO_4$ was synthesized by the solid state reaction, as described in our previous reports.[7,30,31] In a typical synthesis, stoichiometric amounts of the starting materials, $LiOH{\cdot}H_2O$ (Junsei, Japan), Co_3O_4 (Sigma-Aldrich, USA) and $(NH_4)_2HPO_4$ (Sigma-Aldrich, USA), were milled using planetary ball milling for 3 h. The resultant powder was pelletized and heat treated in a box furnace at 400 °C for 10 h to decompose the hydroxyl and ammonia moieties. The final calcination was carried out at 800 °C for 10 h in an air atmosphere to yield $LiCoPO_4$. The obtained $LiCoPO_4$ powders were ground with LiF (Wako, Japan) in a mortar, pelletized and calcined at 650, 700 and 750 °C for 1.5 h under an Ar atmosphere. The samples were cooled down to room temperature by following either natural cooling or a quenching method. The purpose of the quenching process was to prevent the decomposition of the fluorophosphate phase during slow cooling. Additionally, Li_2CoPO_4F powders were synthesized at 700 °C for heating periods of 1, 2 and 4 h following the same quenching synthesis as above, to study the influence of the synthesis duration on the formation of Li_2CoPO_4F materials.

The obtained materials were reground into ultrafine powders and subjected to physical and electrochemical characterizations. The X-ray diffraction pattern of the synthesized powders was recorded using an X-ray diffractometer (XRD, Rint 1000, Rigaku, Japan) with Cu Kα radiation. The surface morphology of the powder was observed using a field emission scanning electron microscope (FE-SEM, S-4700, Hitachi, Japan) equipped with an Energy-dispersive X-ray spectroscope (EDAX) attachment. The CR2032 coin cells were assembled in an argon filled glove box using metallic lithium as the anode and synthesized Li_2CoPO_4F powder as the cathode, which were separated by a porous polypropylene separator (Celgard 3401). The electrolyte used in this study was 1.4 M $LiPF_6$ in ethylene carbonate (EC)/ethyl methyl carbonate (EMC)/ dimethyl carbonate (DMC)/fluoro ethylene carbonate (FEC) (1 : 2 : 6 : 1, v/v ratio) with 2 wt% (TA-218, Soulbrain Co., Ltd., Korea), due to its higher electrochemical stability.[32] The composite cathodes were prepared by pressing preciously weighed 20 mg of active material (Li_2CoPO_4F), 3 mg of Ketzen black (KB) and 3 mg of Teflonized acetylene black (TAB) on a stainless steel current collector and dried at 110 °C for 4 h in a vacuum oven. Galvanostatic charge-discharge tests were performed between 2 and 5.1 V using a battery tester (WBCS 3000, Won-A-Tech, Korea) at room temperature with various current densities. The cyclic voltammograms (CVs) and electrochemical impedance spectroscopy (EIS) spectra were recorded using an electrochemical work station (SP-150, Bio-Logic, France). The CV traces were studied at a scan rate of 0.5 mV s^{-1}, in which lithium served as both the counter and reference electrodes. EIS was carried out after cycling the Li/Li_2CoPO_4F cells at 1 C rate and then de-lithiating at 5.1 V *vs.* Li over the frequency range of 100 kHz to 100 mHz.

Results and discussion

At first, the Li_2CoPO_4F powders were synthesized by heating temperatures at 650, 700 and 750 °C for 1.5 h. The samples were allowed to cool naturally inside the furnace and the final XRD patterns are provided in Fig. 1. From the XRD results, partially formed Li_2CoPO_4F powders were observed at all three temperatures, but their peaks had weak intensities and mixed along with $LiCoPO_4$ impurities phases comprising higher intensity. Other impurity peaks in the XRD patterns are corresponding to unreacted LiF and side reaction product Li_3PO_4 of samples subjected to slow cooling. It means that this natural cooling process is very difficult to obtain well-developed pure Li_2CoPO_4F material. However, there are so many earlier reports of utilizing quenching for effective production of cathode materials for lithium secondary batteries.[33,34] The quenching process favored improvement of initial discharge capacity of the samples and reduced the impurity, which have formed otherwise during the slow cooling process.[35] In this regard, the preparation of Li_2CoPO_4F materials was further investigated by a rapid quenching technique after heating the samples at desired temperatures for 1.5 h.

Fig. 2 represents the powder X-ray diffraction patterns of the Li_2CoPO_4F materials synthesized at various calcination temperatures by a quenching process. The samples showed phase formation at all three temperatures when they were subjected to a heating period of 1.5 h and then quenched to room temperature by directly taking the sample out of furnace after synthesis duration terminates. There is a remarkable

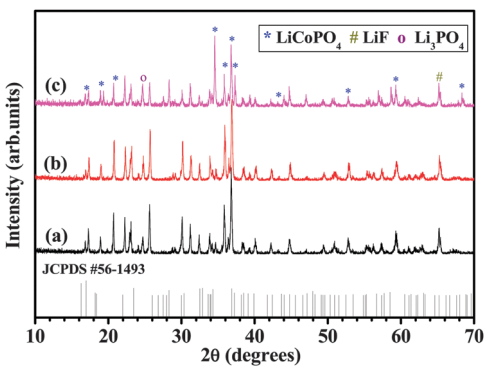

Fig. 1 XRD patterns of Li_2CoPO_4F powders calcined at (a) 650, (b) 700 and (c) 750 °C by slow cooling.

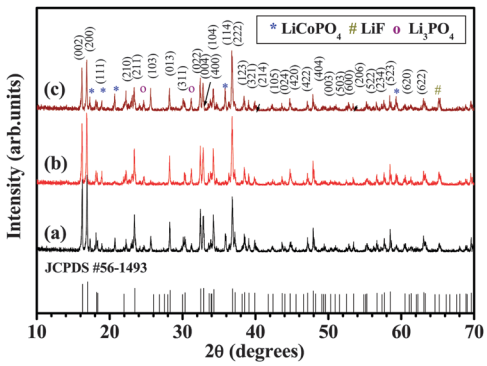

Fig. 2 XRD patterns of Li_2CoPO_4F powders calcined at (a) 650, (b) 700 and (c) 750 °C by quenching.

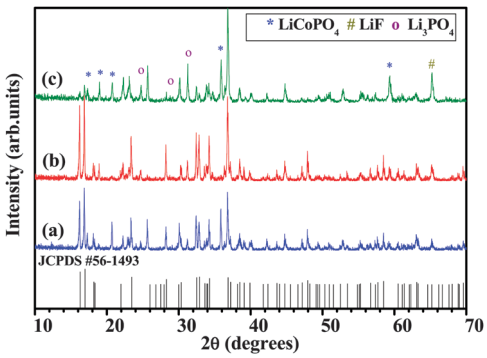

Fig. 3 The influence of the synthesis duration on Li_2CoPO_4F prepared by quenching at 700 °C for (b) 1, (c) 1.5 and (d) 2 h.

difference in the XRD patterns of the quenched samples than those of the slow cooled samples. The characteristic (002) and (200) peaks for Li_2CoPO_4F at 16° and 17° appeared in the quenched samples which was absent completely in the case of slow cooled sample. From the presence of a high level of $LiCoPO_4$ obtained by slow cooled samples (Fig. 1) it can be understood that the Li_2CoPO_4F phase formed at various desirable calcination temperatures, however, it converted and split into $LiCoPO_4$ and LiF during the slow cooling regime; marked by mixed peaks for Li_2CoPO_4F, $LiCoPO_4$ and LiF in Fig. 1(a)–(c). In spite of the phase formation during the synthesis of the Li_2CoPO_4F powders at 650 °C (Fig. 2(a)) and 750 °C (Fig. 2(c)), these samples comprise a comparatively higher level of impurity peaks than the sample synthesized at 700 °C (Fig. 2(b)). The reflections in the XRD patterns of the quenched samples in Fig. 2 were then indexed according to an orthorhombic structure with *Pnma* space group and the obtained patterns are consistent with JCPDS card no. 56-1493. Moreover this Li_2CoPO_4F structure is isostructural with Li_2NiPO_4F.[12,36] The lattice parameters for the 700 °C quenched samples were calculated to be a = 10.462 Å, b = 6.487 Å and c = 10.837 Å and are consistent with the literature values.[22]

In order to verify the influence of the heating duration on the synthesis of the Li_2CoPO_4F material, further investigations were carried out at two different durations, namely 1 and 2 h at 700 °C, for which there were fewer impurities than other samples. The samples were maintained at 700 °C for the above-said durations and then quenched as that of 1.5 h sample. The results obtained for different durations are presented in Fig. 3(a)–(c). It is worth mentioning that increasing the duration of calcination leads to the decomposition of the Li_2CoPO_4F phase, which is clearly evident from the XRD patterns. It is obvious that an increase in the duration of even 30 min from 1.5 to 2 h severely affects the formation of the desired Li_2CoPO_4F phase, as evidenced by the decrease in the intensity of the corresponding XRD peaks. When the heating duration was decreased by 30 minutes from 1.5 h, the effect of sintering is predictable. As expected, there is a clear formation of the Li_2CoPO_4F phase, but with less intensity peaks and more impurities than the corresponding material sintered for 1.5 h. Thus, it can be concurred that a sintering duration of 1.5 h is necessary for high purity crystalline phase formation in the case of Li_2CoPO_4F cathode materials using the above-mentioned starting materials. Similar kinds of reactions were also reported by Wang *et al.*,[25] however the present results contradict those in the previous report by Okada *et al.*,[22] in which they prepared the Li_2CoPO_4F phase by vacuum heating with the same starting materials at about 780 °C for 78 h. Although some impurities were observed in the XRD patterns in the present case, it should be noted that several attempts have been made in the past to synthesize single phase crystalline Li_2CoPO_4F material by using different starting materials, synthesis routes, atmospheric conditions and sintering times. However, all of these procedures ended up with some minor impurity phases, such as Li_3PO_4, $LiCoPO_4$, or LiF. This study and the previous reports clearly indicate that the synthesis of single phase fluorophosphates is complicated, irrespective of the techniques used.[25] From this study, it is revealed that the optimum synthetic condition to yield Li_2CoPO_4F phase is 700 °C for 1.5 h with subsequent quenching.

Fig. 4 shows the surface morphological features of the Li_2CoPO_4F materials synthesized at various temperatures. It can be seen from the SEM images that the synthesized materials exhibited almost uniform sized spherical particulates morphology with average size of 20–50 nm. Partial aggregation of the small sized particles can also be seen in the SEM images. The spherical size and uniform distribution of the particulates can be attributed to the moderate synthesis temperatures with

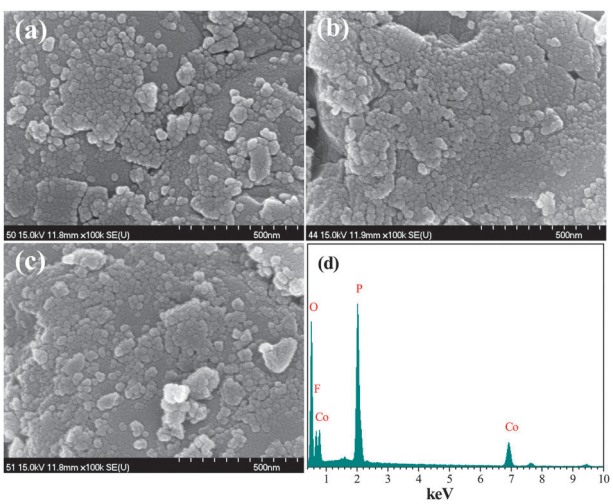

Fig. 4 Scanning electron microscopic images of Li_2CoPO_4F calcined by quenching at (a) 650 °C, (b) 700 °C and (c) 750 °C. (d) Corresponding EDAX pattern of sample synthesized at 700 °C.

short duration. An EDAX analysis was also carried out to ensure the presence of fluorine in the Li_2CoPO_4F synthesized at 700 °C and the results are shown in Fig. 4(d). The P/F ratio was determined by EDAX and found to be 0.17 : 0.16; this value is consistent with the stoichiometric ratio of P/F = 1, which is the same as that of the Co/F ratio.

Galvanostatic cycling performance tests of the Li/Li_2CoPO_4F cells were carried out at a current density of 0.1 mA cm^{-2} between 2 and 5.1 V. The typical charge–discharge curves of the Li/Li_2CoPO_4F cells are presented in Fig. 5(a). The test cells delivered an initial reversible capacity of 117, 132, and 91 mA h g^{-1} for the materials prepared at 650, 700 and 750 °C, respectively. At the same time, in all of the cases, the charge capacity exceeds the theoretical capacity (144 mA h g^{-1}) for the one electron reaction. Due to the restricted operating potential of the electrolyte solution, two electron reactions are not plausible, in other words the $Co^{3+/4+}$ redox couple is not feasible. Hence, the excess capacity is mainly ascribed to the decomposition of the electrolyte solution used at higher potentials. It is interesting to note that 92% of the theoretical capacity for one electron transfer could be achieved by adopting the new 1.4 M $LiPF_6$ in EC/EMC/DMC/FEC electrolyte solution for the 700 °C quenched sample. It is believed that the presence of the FEC component in the electrolyte solution as a co-solvent/additive substantially improves the cyclability of the cell. Also, fluorinated-carbonate has excellent film forming properties and better de-solvation characteristics, which decrease the interfacial solid electrolyte interphase (SEI) film resistance and facilitate the lithium ion diffusion across the film. More clearly, the incorporation of FEC slows down the oxidation process of solvent molecules (EC, EMC and DMC) at high potential charging, which in turn provides better cyclability

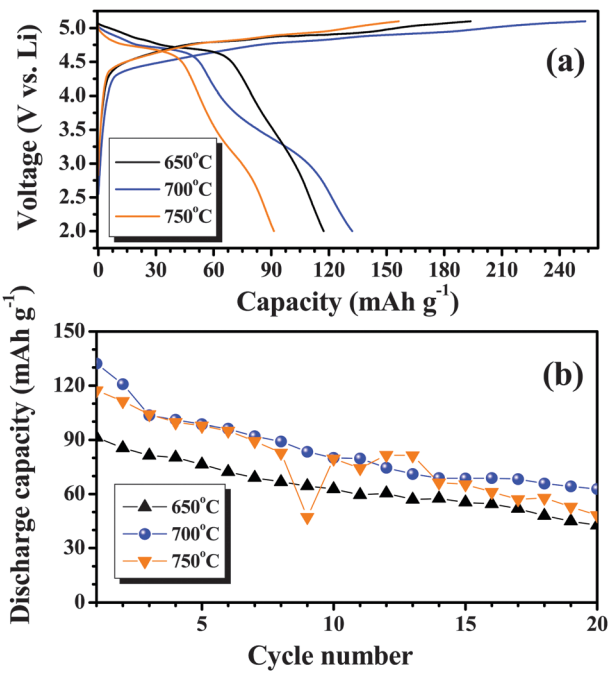

Fig. 5 Electrochemical performances of Li/Li_2CoPO_4F cells cycled between 2–5.1 V *vs.* Li at 0.08 C in room temperature. (a) Initial charge-discharge curves and (b) corresponding cycle performance of the above cells.

than additive free electrolytes (see Fig. S1, ESI†).[37–39] Furthermore, the FEC component increases the Li intercalation kinetics through the formation of a film with lower interfacial impedance during charge–discharge, thus preventing Li plating on the anodes under low temperature conditions. Interestingly, the fluorinated electrolyte has low flammability and the resulting Li-ion cell can therefore be made safer. The monotonous discharge curve represents the single phase electrochemical reaction, which is consistent with the previous report by Okada *et al.*[22] Further, the initial reversible capacity of 132 mA h g^{-1} is much higher than that reported elsewhere for Li_2CoPO_4F material.[22,23,25,40] The effect of the optimum calcination temperature on the cycle performance is observed in Fig 5(b). The materials prepared at all three temperatures showed almost the same decrease in their capacity values. Among them, the Li_2CoPO_4F phase prepared at 700 °C exhibited the highest capacity retention of over 50% during cycling, which is higher than those of the phases prepared at 650 and 750 °C. The enhanced performance of this phase is mainly ascribed to the smaller particle size, relatively high purity with fewer impurities, moderate temperature of synthesis and careful selection of the electrolyte.

Li/Li_2CoPO_4F cells were galvanostatically cycled at different current rates in the range of 2–5.1 V and the results are presented in Fig. 6. The cells showed initial discharge capacities of 129, 119 and 108 mA h g^{-1} for 0.2, 0.5 and 1 C rates, respectively. It is obvious that the discharge profile curves obtained at all three current rates are similar to each other. As expected, the discharge capacity tends to decrease with increasing current rate and this may be explained by the fact that at high current rates the electrochemical reaction takes place only on the surface rather than in the bulk.[41] The cycling performances of the Li/Li_2CoPO_4F cells are illustrated in Fig. 6(b). At all three current rates, the discharge capacities tend to fade, which may be due to the poor compatibility with the electrolyte solutions and surface erosion of the cathode particles. After 15 cycles, 41, 37 and 40% of the initial discharge capacities are retained for 0.2, 0.5 and 1 C rates, respectively. In spite of using a sulfolane-based electrolyte,[25] which was believed to be stable up to 5.5 V *vs.* Li, and a higher upper cut off potential than the current study, the capacity obtained was 109 mA h g^{-1} that is almost the same as obtained at the 1 C rate for a upper cut off potential of 5.1 V for the quenched sample synthesized at 700 °C. To the best of our knowledge, the cycling result obtained in this study is one of the best results obtained so far for Li/Li_2CoPO_4F cells tested at high current densities, especially under 1 C rate test conditions.[42] The effect of high current rate on the internal resistance of the materials in a cell cycled for 15 cycles was further analyzed by electrochemical impedance spectroscopy.

Accordingly, EIS analysis was carried out to check the diffusion of the current into the surface of the cathode after high current rate cycling. The cells were charged to 5.1 V *vs.* Li after cycling at 1 C rate for 15 cycles. The EIS spectra for the de-lithiated cells were recorded once the current reached 1 C equivalent. An equivalent circuit model corresponding to the impedance data was obtained. The circuit and the fitted data are also provided along with the experimental data in Fig. 7. Each Nyquist plot showed a semicircle in the high frequency

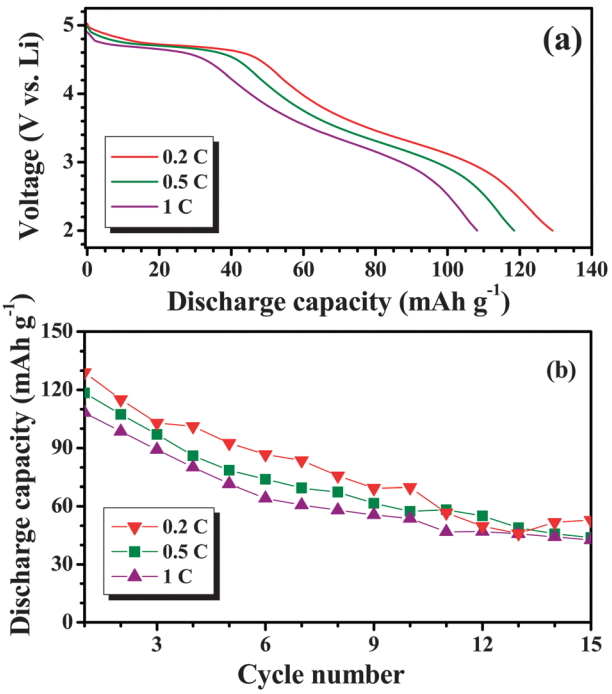

Fig. 6 Rate performance of Li/Li_2CoPO_4F cells with sample prepared at 700 °C (a) Initial discharge curves and (b) corresponding cycling performance.

region and a sloping line in the low frequency region, which is common for cathode materials used in lithium secondary batteries. The intercept of the semicircle at the high frequency region corresponds to Ohmic resistance of the cell. The semicircle in the high frequency region can be ascribed to the charge transfer resistance related to the lithium ion transfer at the electrolyte–cathode interface and the inclined line in the low frequency region is due to the Warburg impedance responsible for solid state Li–ion diffusion into the bulk of the Li_2CoPO_4F cathode materials. Moreover, the small magnitude of the charge transfer resistance for the sample prepared at 700 °C compared with that of the sample prepared at 750°C indicates fast reaction kinetics, even after 15 cycles at a high current rate. These fast reaction kinetics are due to the high

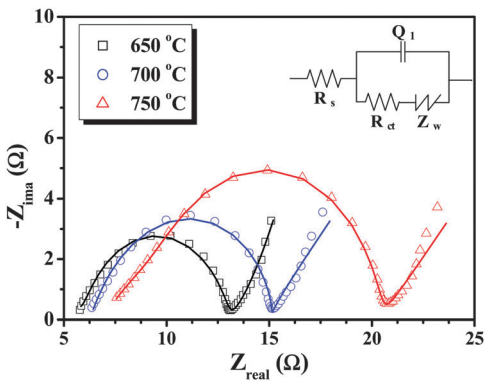

Fig. 7 Nyquist plots of de-lithiated cells at 1 C rate after 15 cycles containing Li_2CoPO_4F prepared at different temperatures. The fitted line for experimental data (symbols) with the equivalent circuit used for fitting was also displayed.

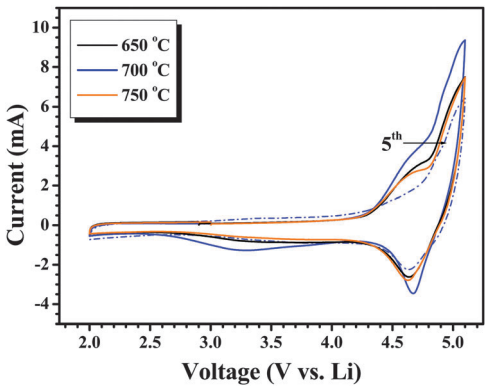

Fig. 8 Cyclic voltammogram of Li/Li_2CoPO_4F cell recorded between 2 and 5.1 V *vs.* Li with scan rate of 0.5 mV s^{-1} for samples synthesized at different temperatures. All of the continuous lines represent the 1st cycle and the dashed lines represent the 5th cycle of the sample prepared at 700 °C.

reaction surface area induced by the small particle size (Fig. 4), which in turn improves the lithium diffusion capability by decreasing the diffusion path within the Li_2CoPO_4F particles and also due to the less impurities indicated in the XRD pattern.

In addition, cyclic voltammetry (CV) analysis was performed to study the electrochemical insertion and extraction behavior of Li^+ ions for all of the samples. The CV traces were recorded between 2–5.1 V *vs.* Li at a scan rate of 0.5 mV s^{-1} in a two electrode coin cell configuration and are shown in Fig. 8. For the CV measurements, metallic lithium acts as both the counter and reference electrodes. In the first cycle, the two oxidative peaks at ~4.8 V and ~5.1 V correspond to the extraction of lithium in two steps from the crystal lattice, whereas insertion takes place in a single step with a broad potential at ~4.67 V *vs.* Li. The maximum heights of the anodic and cathodic peak currents were observed for the sample prepared at 700 °C, while for the other samples both peak currents had almost the same height and were lower than those of the sample prepared at 700 °C. This indicates the superior charge–discharge capability of the sample prepared at 700 °C. The observed CV traces are consistent with the previous reports by Khasanova *et al.*[24] and Okada *et al.*[22] A structural transformation takes place upon the first de-intercalation and insertion, which is clearly evident from the deviation of the CV traces in the subsequent cycles (dashed line in Fig. 8). Furthermore, the smooth oxidation and reduction curves confirm that the Li-insertion and extraction reaction occurred in a single phase reaction, unlike the two-phase reaction mechanism in $LiCoPO_4$.[43] The observed CV data are in good agreement with the galvanostatic charge–discharge profile. Overall, the electrochemical performance of the synthesized Li_2CoPO_4F is similar to that of $LiCoPO_4$ and further studies are in progress to improve its cycling performance by adopting various strategies, including high voltage electrolytes, surface modification, metal doping and so on.

Conclusion

Lithium cobalt fluorophosphate (Li_2CoPO_4F) was successfully synthesized by the conventional solid state reaction method by

a two-step process. Quenching the samples after the final sintering period was helpful in the formation of pure phase Li_2CoPO_4F cathode materials. The development of the Li_2CoPO_4F phase with some minor impurity phases was confirmed by X-ray diffraction measurements. Spherical shape morphology was noted for the synthesized Li_2CoPO_4F powders. For the electrochemical measurements, 1.4 M $LiPF_6$ in the EC/EMC/DMC/FEC electrolyte was used between 2 and 5.1 V *vs*. Li at room temperature. A Li/Li_2CoPO_4F cell exhibited an initial discharge capacity of 132 mA h g^{-1} which is 92% of the theoretical capacity for one electron transfer as well as a superior high rate performance at the 1 C rate. A high capacity of 108 mA h g^{-1} was obtained at the 1 C rate and it can be attributed to the less charge transfer resistance obtained during impedance measurement. Cyclic voltammetry clearly revealed that the Li-insertion/extraction reaction was observed in a single phase reaction, unlike that of the bi-phase reaction in $LiCoPO_4$.

Acknowledgements

This work was supported by the National Research Foundation of Korea Grant funded by the Korean Government (MEST) (NRF-2011-C1AAA001-0030538).

References

1 J. M. Tarascon and M. Armand, *Nature*, 2001, **414**, 359–367.
2 J. B. Goodenough and Y. Kim, *Chem. Mat.*, 2009, **22**, 587–603.
3 M.-K. Song, S. Park, F. M. Alamgir, J. Cho and M. Liu, *Mat. Sci. Eng.: R: Reports*, 2011, **72**, 203–252.
4 V. Aravindan, J. Gnanaraj, S. Madhavi and H.-K. Liu, *Chem. –Eur. J.*, 2011, **17**, 14326–14346.
5 O. K. Park, Y. Cho, S. Lee, H.-C. Yoo, H.-K. Song and J. Cho, *Energy & Environ. Sci.*, 2011, **4**, 1621–1633.
6 A. K. Padhi, K. S. Nanjundaswamy and J. B. Goodenough, *J. Electrochem. Soc.*, 1997, **144**, 1188–1194.
7 I. C. Jang, C. G. Son, S. M. G. Yang, J. W. Lee, A. R. Cho, V. Aravindan, G. J. Park, K. S. Kang, W. S. Kim, W. I. Cho and Y. S. Lee, *J. Mat. Chem.*, 2011, **21**, 6510–6514.
8 S. B. Lee, I. C. Jang, H. H. Lim, V. Aravindan, H. S. Kim and Y. S. Lee, *J. Alloys and Compounds*, 2010, **491**, 668–672.
9 H. H. Lim, I. C. Jang, S. B. Lee, K. Karthikeyan, V. Aravindan and Y. S. Lee, *J. Alloys and Compounds*, 2010, **495**, 181–184.
10 C. G. Son, H. M. Yang, G. W. Lee, A. R. Cho, V. Aravindan, H. S. Kim, W. S. Kim and Y. S. Lee, *J. Alloys and Compounds*, 2011, **509**, 1279–1284.
11 A. R. Cho, J. N. Son, V. Aravindan, H. Kim, K. S. Kang, W. S. Yoon, W. S. Kim and Y. S. Lee, *J. Mat. Chem.*, 2012, **22**, 6556–6560.
12 M. Dutreilh, C. Chevalier, M. El-Ghozzi, D. Avignant and J. M. Montel, *J. Solid State Electrochem.*, 1999, **142**, 1–5.
13 B. L. Ellis, W. R. M. Makahnouk, Y. Makimura, K. Toghill and L. F. Nazar, *Nat. Mater.*, 2007, **6**, 749–753.
14 G. G. Amatucci and N. Pereira, *J. Fluorine Chem.*, 2007, **128**, 243–262.
15 P. Barpanda, J.-N. l. Chotard, N. Recham, C. Delacourt, M. Ati, L. Dupont, M. Armand and J.-M. Tarascon, *Inorganic Chem.*, 2010, **49**, 7401–7413.
16 J. Barker, M. Y. Saidi, R. K. B. Gover, P. Burns and A. Bryan, *J. Power Sources*, 2007, **174**, 927–931.
17 Y. Makimura, L. S. Cahill, Y. Iriyama, G. R. Goward and L. F. Nazar, *Chem. Mater.*, 2008, **20**, 4240–4248.
18 T. N. Ramesh, K. T. Lee, B. L. Ellis and L. F. Nazar, *Electrochem. Solid-State Lett.*, 2010, **13**, A43–A47.
19 N. Recham, J. N. Chotard, J. C. Jumas, L. Laffont, M. Armand and J. M. Tarasco, *Chem. Mater.*, 2010, **22**, 1142–1148.
20 S.-W. Kim, D.-H. Seo, H. Kim, K.-Y. Park and K. Kang, *Phys. Chem. Chem. Phys.*, 2012, **14**, 3299–3303.
21 B. L. Ellis, W. R. M. Makahnouk, W. N. Rowan-Weetaluktuk, D. H. Ryan and L. F. Nazar, *Chem. Mater.*, 2009, **22**, 1059–1070.
22 S. Okada, M. Ueno, Y. Uebou and J.-i. Yamaki, *J. Power Sources*, 2005, **146**, 565–569.
23 E. Dumont-Botto, C. Bourbon, S. Patoux, P. Rozier and M. Dolle, *J. Power Sources*, 2011, **196**, 2274–2278.
24 N. R. Khasanova, A. N. Gavrilov, E. V. Antipov, K. G. Bramnik and H. Hibst, *J. Power Sources*, 2011, **196**, 355–360.
25 D. Wang, J. Xiao, W. Xu, Z. Nie, C. Wang, G. Graff and J.-G. Zhang, *J. Power Sources*, 2011, **196**, 2241–2245.
26 M. Armand, F. Endres, D. R. MacFarlane, H. Ohno and B. Scrosati, *Nat. Mater.*, 2009, **8**, 621–629.
27 A. Lewandowski and A. Świderska-Mocek, *J. Power Sources*, 2009, **194**, 601–609.
28 M. Galiński, A. Lewandowski and I. Stępniak, *Electrochim. Acta*, 2006, **51**, 5567–5580.
29 Y. L. Cheah, N. Gupta, S. S. Pramana, V. Aravindan, G. Wee and M. Srinivasan, *J. Power Sources*, 2011, **196**, 6465–6472.
30 K. Karthikeyan, V. Aravindan, S. B. Lee, I. C. Jang, H. H. Lim, G. J. Park, M. Yoshio and Y. S. Lee, *J. Power Sources*, 2010, **195**, 3761–3764.
31 I. C. Jang, C. G. Son, S. M. G. Yang, J. W. Lee, A. R. Cho, V. Aravindan, G. J. Park, K. S. Kang, W. S. Kim, W. I. Cho and Y. S. Lee, *J. Mater. Chem.*, 2011, **21**, 6510–6514.
32 R. McMillan, H. Slegr, Z. X. Shu and W. Wang, *J. Power Sources*, 1999, **81–82**, 20–26.
33 Z. Lu, D. D. MacNeil and J. R. Dahn, *Electrochem. and Solid-State Lett.*, 2001, **4**, A200–A203.
34 R. Thomas J, *J. Power Sources*, 2003, **119–121**, 262–265.
35 H. Lin, J. Zheng and Y. Yang, *Mater. Chem. Phys.*, 2010, **119**, 519–523.
36 M. Nagahama, N. Hasegawa and S. Okada, *J. Electrochem. Soc.*, 2010, **157**, A748–A752.
37 R. Mogi, M. Inaba, S.-K. Jeong, Y. Iriyama, T. Abe and Z. Ogumi, *J. Electrochem. Soc.*, 2002, **149**, A1578–A1583.
38 N.-S. Choi, K. H. Yew, K. Y. Lee, M. Sung, H. Kim and S.-S. Kim, *J. Power Sources*, 2006, **161**, 1254–1259.
39 Z. Sheng Shui, *J. Power Sources*, 2006, **162**, 1379–1394.
40 J. Barker, R. K. B. Gover, P. Burns, A. Bryan, M. Y. Saidi and J. L. Swoyer, *J. Electrochem. Soc.*, 2005, **152**, A1776–A1779.
41 K. Zaghib, J. B. Goodenough, A. Mauger and C. Julien, *J. Power Sources*, 2009, **194**, 1021–1023.
42 N. V. Kosova, E. T. Devyatkina and A. B. Slobodyuk, *Solid State Ionics*, 2011, DOI: 10.1016/j.ssi.2011.11.007.
43 N. N. Bramnik, K. G. Bramnik, C. Baehtz and H. Ehrenberg, *J. Power Sources*, 2005, **145**, 74–81.